



THE UNIVERSITY *of* EDINBURGH

Edinburgh Research Explorer

## Evolution of the Yellow River Delta and its relationship with runoff and sediment load from 1983 to 2011

**Citation for published version:**

Borthwick, A, Kong, D, Miao, C, Duan, C, Liu, H, Sun, Q, Ye, A, Di, Z & Gong, W 2015, 'Evolution of the Yellow River Delta and its relationship with runoff and sediment load from 1983 to 2011', *Journal of Hydrology*, vol. 520, pp. 157-167. <https://doi.org/10.1016/j.jhydrol.2014.09.038>

**Digital Object Identifier (DOI):**

[10.1016/j.jhydrol.2014.09.038](https://doi.org/10.1016/j.jhydrol.2014.09.038)

**Link:**

[Link to publication record in Edinburgh Research Explorer](#)

**Document Version:**

Peer reviewed version

**Published In:**

Journal of Hydrology

**General rights**

Copyright for the publications made accessible via the Edinburgh Research Explorer is retained by the author(s) and / or other copyright owners and it is a condition of accessing these publications that users recognise and abide by the legal requirements associated with these rights.

**Take down policy**

The University of Edinburgh has made every reasonable effort to ensure that Edinburgh Research Explorer content complies with UK legislation. If you believe that the public display of this file breaches copyright please contact [openaccess@ed.ac.uk](mailto:openaccess@ed.ac.uk) providing details, and we will remove access to the work immediately and investigate your claim.



## Accepted Manuscript

Evolution of the Yellow River Delta and its relationship with runoff and sediment load from 1983 to 2011

Dongxian Kong, Chiyuan Miao, Alistair G.L. Borthwick, Qingyun Duan, Hao Liu, Qiaohong Sun, Aizhong Ye, Zhenhua Di, Wei Gong

PII: S0022-1694(14)00720-3

DOI: <http://dx.doi.org/10.1016/j.jhydrol.2014.09.038>

Reference: HYDROL 19899

To appear in: *Journal of Hydrology*

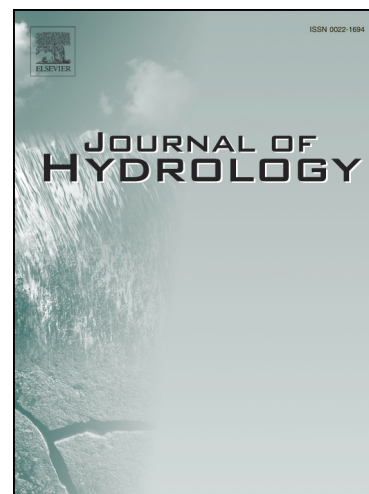
Received Date: 22 May 2014

Revised Date: 5 August 2014

Accepted Date: 14 September 2014

Please cite this article as: Kong, D., Miao, C., Borthwick, A.G.L., Duan, Q., Liu, H., Sun, Q., Ye, A., Di, Z., Gong, W., Evolution of the Yellow River Delta and its relationship with runoff and sediment load from 1983 to 2011, *Journal of Hydrology* (2014), doi: <http://dx.doi.org/10.1016/j.jhydrol.2014.09.038>

This is a PDF file of an unedited manuscript that has been accepted for publication. As a service to our customers we are providing this early version of the manuscript. The manuscript will undergo copyediting, typesetting, and review of the resulting proof before it is published in its final form. Please note that during the production process errors may be discovered which could affect the content, and all legal disclaimers that apply to the journal pertain.



1 **Evolution of the Yellow River Delta and its relationship with runoff and sediment**  
2 **load from 1983 to 2011**

3 Dongxian Kong<sup>1</sup>, Chiyuan Miao<sup>1,2\*</sup>, Alistair G.L. Borthwick<sup>3</sup>, Qingyun Duan<sup>1</sup>, Hao Liu<sup>4</sup>, Qiaohong  
4 Sun<sup>1</sup>, Aizhong Ye<sup>1</sup>, Zhenhua Di<sup>1</sup>, Wei Gong<sup>1</sup>

5 <sup>1</sup>State Key Laboratory of Earth Surface Processes and Resource Ecology, College of Global  
6 Change and Earth System Science, Beijing Normal University, Beijing 100875, P.R.China

7 <sup>2</sup>Yellow River Institute of Hydraulic Research, Key Laboratory of Soil and Water Loss Process and  
8 Control on the Loess Plateau of Ministry of Water Resources, Zhengzhou, Henan, 450003

9 <sup>3</sup>School of Engineering, The University of Edinburgh, The King's Buildings, Edinburgh EH9 3JL,  
10 U.K.

11 <sup>4</sup>Department of Civil and Environmental Engineering, University of California, Irvine, CA 92697,  
12 USA

13  
14  
15 **Abstract:** Long-term data from a hydrological monitoring station and remotely-sensed satellite  
16 images were used to explore the effects of runoff and suspended sediment load on evolution of the  
17 Yellow River Delta (YRD) from 1983 to 2011. During this period, an average runoff of  $18.0 \times 10^9$   
18  $\text{m}^3 \text{yr}^{-1}$  and an average sediment load of  $341 \times 10^6 \text{ t yr}^{-1}$  flowed through the delta lobes into the sea.  
19 The runoff and sediment load exhibited downward trends with time, along with large inter-annual  
20 fluctuations. Three stages were evident in the data. From 1983 to the late 1990s, the Yellow River  
21 experienced progressively severe droughts which reduced both runoff and sediment load to its delta  
22 lobe. The delta nevertheless grew to a peak area of about  $3950 \text{ km}^2$  in 2000. From 2000 to 2003,  
23 the YRD area decreased. Meanwhile, the operation of the dam at Xiaolangdi and changes in water  
24 consumption driven by a new regulatory framework helped stabilize the runoff. Although the  
25 sediment load continued to decline, partly due to sediment check dams along the middle Yellow  
26 River and the reduced sediment carrying capacity of the river, the YRD area nevertheless increased  
27 between 2003 and 2011. The variations in runoff and sediment load directly influenced changes to

---

\* Corresponding authors. Tel.: +86-10-58804191; fax: +86-10-58804191.

*E-mail address:* miaocy@vip.sina.com (C. Miao)

28 the plan-form area, shoreline migration, and morphology of the YRD. From 1983 to 2011, the net  
29 land area of the delta increased by 248 km<sup>2</sup>, its coastline extended by 36.45 km, and its shape  
30 became increasingly irregular due to the emergence of its delta lobes. In 1996, an artificial  
31 diversion altered the position of the main delta lobe from Qingshuigou to Qing 8. A stepwise  
32 multiple regression analysis indicated that the YRD would have required average sediment loads of  
33 about  $441 \times 10^6 \text{ t yr}^{-1}$  before 1996 and  $159 \times 10^6 \text{ t yr}^{-1}$  after 1996 to maintain equilibrium.

34

35 **Keywords:** delta; Yellow River; climate change; human activity

36

37

## 38 1. Introduction

39 A river delta is formed by the deposition of river sediment as it enters the sea. Deltas  
40 simultaneously respond to environmental change by shrinking and expanding over temporal and  
41 spatial scales. Both the runoff and sediment load delivered to the sea are dominant factors affecting  
42 the evolution of a delta (Yu et al., 2011). Climate change has a direct affect on river delta systems  
43 by altering the upstream runoff (Xu, 2005; Wang et al., 2012; Gao et al., 2012). Furthermore,  
44 human activities, such as water diversion works, reservoir dam constructions, and soil and water  
45 conservation measures (e.g. sediment check dams, contour farming, afforestation, land  
46 consolidation, and water pricing) can also radically alter delta ecosystems by influencing the  
47 quantities of water and sediment discharging into the sea through the delta lobes (Xu, 2005; Miao et  
48 al., 2010; Wang et al., 2012; Gao et al., 2014a, 2014b). In recent decades, almost all river deltas  
49 around the world have been impacted upon by human activities, and the increased frequency and  
50 severity of extreme runoff events through climate variability and change. Examples include deltas  
51 in the Nile river (El Banna and Frihy, 2009), Ebro River (Mikhailova, 2003), Mississippi River  
52 (Snedden et al., 2007), Mekong River (Le et al., 2007), Yangtze River (Yang et al., 2011), Pearl  
53 River (Zhang et al., 2010) and Yellow River (Wang et al., 2010). Recent research has established  
54 that 85% of the river deltas around the world shrank during the first decade of 21<sup>st</sup> Century duo to  
55 sediment capture in the upstream reaches of their river basins, and it is believed that this situation  
56 will become more severe in the future (Syvitski et al., 2009).

57 The Yellow River Delta (YRD) provides one of the most poignant examples worldwide of the  
58 huge impacts on a delta that can arise from increased droughts and human activities affecting water  
59 consumption, river regulation, soil conservation, etc. (Miao and Ni, 2009). As the birthplace of  
60 ancient Chinese civilization, the lower Yellow River was the most prosperous region in early  
61 Chinese history (Yu, 2002) and remains of major socio-economic importance in modern China. The  
62 Yellow River is the second largest river in the world in terms of sediment load, with an average of  
63  $1.1 \times 10^9 \text{ t yr}^{-1}$  reaching the ocean annually (Milliman and Meade, 1983). Approximately 30 – 40 %  
64 of the sediment transported to the sea is deposited at the delta lobe at the mouth of the Yellow River,  
65 forming the YRD (Li et al., 1998). Over the past 30 years, many research studies have been carried  
66 out on the YRD due to its socio-economic importance and unique ecological environment (Cui et  
67 al., 2009). For example, the YRD contains the second largest oilfield in China (Shengli Oilfield). It  
68 is also rich in biological resources and is home to 1,543 wild animal species, 393 seed plant species,

69 and 283 bird species (including 9 species qualifying as first-level nationally protected birds, and 42  
70 at the second level) (Zhang et al., 1998). The YRD wetland is an important habitat and transfer area  
71 for many rare and endangered migrating birds, such as the red-crowned crane, hooded crane,  
72 Siberian crane, oriental stork, black stork, and golden eagle (Xu et al., 2002). In recent decades, the  
73 combination of decreasing runoff and sediment load due to increasing occurrences and severity of  
74 low-flow events (Yang et al., 1998) exacerbated by the influence of human activities (Fan et al.,  
75 2006a) have led to significant modifications to the YRD, including changes to its wetland  
76 landscape, biodiversity and deltaic configuration (Cui et al., 2013; Higgins et al., 2013).

77 Previous studies primarily focused on the qualitative relationship between the evolution of  
78 YRD and the stream-flow and sediment load in the delta lobe (Chu et al., 2006; Peng et al., 2010;  
79 Wang et al., 2010; Yu et al., 2011), land-use of the YRD (Chen et al., 2011; Zhang et al., 2011;  
80 Miao et al., 2012b; Ottinger et al., 2013), and shoreline changes (Cui and Li, 2011; Yang, 2012; Liu  
81 et al., 2013). Less attention was paid to quantitative contribution of runoff and sediment load on the  
82 YRD, the influence of artificial shifts of the course of the main delta lobe channel on the overall  
83 balance of the YRD, and the impacts of drought and human activities in the Yellow River basin on  
84 the evolution of YRD.

85 The aim of the present study is to examine the evolution of the Yellow River delta from 1983  
86 to 2011 during which major droughts occurred (due to a combination of reduced runoff caused by  
87 climate change, increased water consumption driven by population change, rapid socio-economic  
88 development and poor irrigation practice), an artificial diversion of the delta lobe was implemented,  
89 a major reservoir began operation for flushing sediment and flood control, and changes that took  
90 place in regulation practice by the Yellow River Conservancy Commission from water and soil  
91 conservancy to an integrated framework. The YRD therefore provides a very useful exemplar to  
92 scientists, engineers, environmentalists and decision makers as a case study of the effects of  
93 drought-driven and anthropogenic changes to a key river delta. This paper analyzes the variations  
94 in runoff and sediment load in the Yellow River, and their effect on the morphological evolution of  
95 the delta. An assessment is made of the threshold values of sediment load required to main the  
96 equilibrium of the delta before and after artificial diversion led to a new delta lobe at Qing 8 in  
97 1996. An error analysis is included. The insights gained about the temporal behavior of the YRD  
98 should be useful to decision makers weighing up future options for large-scale constructions and  
99 environmental protection measures affecting the YRD.

100

101 **2. Yellow River Delta: study area, event chronology, and data sources**

## 102 2.1. Study area

103 The YRD is located in the northeast of Shandong Province, China (Figure 1). The northern  
104 and eastern portions of the YRD are adjacent to the Bohai Sea and Laizhou Bay. Three large  
105 artificial diversions of the main channel in the YRD were implemented in the past five decades  
106 (Fan et al., 2006b; Syvitski and Saito, 2007). In July 1964, the course of the Yellow River delta lobe  
107 was altered artificially from the Shenxiangou route to the Diaokou course to help alleviate potential  
108 flood problems. In May 1976, development of the Shengli Oilfield caused the delta lobe to shift  
109 course into the Bohai Sea through the Qingshuigou River. In August 1996, the main channel of the  
110 delta lobe was diverted northeast to the 8<sup>th</sup> section of the Qingshuigou River forming the Qing 8  
111 course (Xu et al., 2002) in order to facilitate the offshore to onshore operation of the Xintan and  
112 Kendong Oilfields. Since then, the course of the delta lobe of the Yellow River has remained  
113 essentially unchanged, apart from some minor movements.

114

115 **Figure 1**

116

117 The YRD region is characterized by a warm-temperate continental monsoon climate with  
118 distinct seasons (Sun et al., 2014). The annual mean temperature ranges from 11.5 to 12.4 °C, with  
119 highest monthly temperature of 26.6 °C in July and lowest of -4.1 °C in January. The YRD is  
120 located in a semi-arid zone where the annual rainfall is 590.9 mm and pan evaporation exceeds  
121 1500 mm. The monthly maximum rainfall is 227 mm in July and the minimum rainfall is 1.7 mm in  
122 January. Approximately 70% of the total annual precipitation occurs in the summer. Dominant soil  
123 types are alluvial and saline (Fang et al., 2005). Sediment in the Yellow River discharging into the  
124 sea has a composition of between 8-28 % sand, 64-78 % silt, and 6-21 % mud (Lim et al. 2006).  
125 Sediment transport is primarily as suspended sediment. There is almost no bed load in the Yellow  
126 River. The median grain size of the suspended sediment is 0.015-0.025 mm at Lijin station (Xu,  
127 2000). Natural vegetation in the YRD primarily comprises *Phragmites australis*, *Suaeda*  
128 *heteroptera*, *Tamarix chinensis*, *Triarrhena sacchariflora*, *Myriophyllum spicatum*, and *Limonium*  
129 *sinense* (Jiang et al., 2013).

130

131 2.2. Chronology of hydrological and human impacts on the Yellow River from 1983-2011

132 The lower Yellow River experienced substantial hydrological and human impacts during the  
133 study period. From the 1970s to the late 1990s, the river suffered increasingly severe droughts,  
134 during which progressively increasing numbers of no-flow and nearly no-flow events occurred  
135 close to the delta mouth. El Niño/Southern Oscillation (ENSO) events affected the strength of  
136 monsoons passing over the Tibetan plateau where the source catchment is located. The drought  
137 events were caused by a combination of factors including climate change leading to increased  
138 temperature and decreased precipitation in the upper catchment areas, poor irrigation practice along  
139 the middle reaches, and increased water consumption linked to enhanced socio-economic  
140 development and some population growth. Man-made constructions also had a major effect on  
141 the lower Yellow river and YRD, in particular the artificial diversion of the delta lobe in 1996 and  
142 the construction from 1994 to 2000 and operation from about 2000 of the reservoir-dam at  
143 Xiaolangdi. By 2000, the condition of the lower Yellow River was a major national concern in  
144 China, considerable investment was made into remediation of the lower Yellow River, and the  
145 Yellow River Conservancy Commission altered its approach from a conservancy framework related  
146 to flood control (e.g. Yellow River Water Allocation Plan in 1987) to an integrated one of  
147 sustainability involving water saving and water pricing policies (Li, 2003). Since 2000, the  
148 Yellow River has flowed continuously to the sea, but there remain major concerns about its vitality.

149

150 2.3. Data sources

151 The study utilized multi-temporal remotely-sensed Landsat data from a Multispectral Scanner  
152 (MSS), a Thematic Mapper (TM) and an Enhanced Thematic Mapper (ETM+) obtained in the  
153 period from 1983 to 2011, totaling 29 scenes (Table 1) archived by the Earth Resources  
154 Observation and Science (EROS) Center (<http://glovis.usgs.gov/>). All data accounted for the impact  
155 of cloud cover. The spatial resolution of the MSS, TM and ETM+ data were 80 m, 30 m and 30 m  
156 (Tucker et al., 2004; Chander et al., 2009). According to the Worldwide Reference System, one full  
157 MSS (path 130, row 34) or TM (path 121, row 34) scene fully covered the study area. Data on  
158 annual runoff and suspended sediment load at selected hydrological stations from 1983 to 2011  
159 were obtained from the Yellow River Conservancy Commission (YRCC). The annual regional  
160 precipitation series were interpolated from data from 175 meteorological stations, which were

161 provided by the National Meteorological Information Center of the China Meteorological  
162 Administration.

163

164 **Table 1**

165

### 166 **3. Methodology**

167 In practice, coastline extraction methods include manual photointerpretation techniques by  
168 experts, and computational methods such as edge-detection (Lee and Jurkevich, 1990; Mason and  
169 Davenport, 1996), neural networks (Ryan et al., 1991), locally adaptive thresholding (Liu and Jezek,  
170 2004), fuzzy connectivity (Dellepiane et al., 2004), mathematical morphology (Geleynse et al.,  
171 2012) and pulse coupled neural networks (Del Frate et al., 2012). The present study applied an  
172 interactive interpretation technique combining an automatic boundary detection algorithm with  
173 human supervision to detect the land-ocean shoreline boundaries in satellite images. The automatic  
174 boundary detection procedure consisted of four steps. First, we calculated the background trend to  
175 remove specular reflection of solar radiation on non-flat water surfaces. Second, we applied a  
176 noise-removing algorithm to reduce scattered noise contaminating the satellite images. Third, we  
177 chose adaptively a threshold that differentiated the land from the ocean, and then transformed the  
178 data into black-white (BW) binary form. Finally, we employed an automatic boundary-detection  
179 algorithm to locate boundaries in the BW-images, and verified or adjusted them with reference to a  
180 combined TM 432 pseudo-color image. MatLab(R) and its Image Processing Toolbox were used to  
181 implement the algorithm and batch-process all the Landsat imageries.

182 Provided the distributary channels are free to migrate across a delta plain, then widespread  
183 sedimentation occurs (Syvitski et al., 2009). This means that a river delta tends to be part of circle,  
184 if without artificial control. It is well-established that the YRD is a typical fan-shaped delta (Sun et  
185 al., 2002; Chu et al., 2006). The radius of the circle can be calculated from either its area as  $R_S$  or its  
186 perimeter as  $R_L$ . Variations in  $R_S$  and  $R_L$  represent changes to the river delta. An increase in  $R_S$   
187 indicates accretion of the delta area, whereas a decrease indicates erosion. An increase in  $R_L$   
188 indicates extension of the coastline, whereas a decrease indicates shortening. The delta radius ratio,  
189  $R_S / R_L$ , can be used to characterize the morphology of the YRD. A value close to 1 indicates the  
190 shoreline follows a nearly smooth arc, and thus the delta is developing in a spatially uniform  
191 manner. A value well away from 1 indicates a tortuous shoreline and that the delta is developing an

192 irregular shape. Values for  $R_S$ ,  $R_L$  and the radius ratio are determined using the following formulas:

$$193 \quad R_S = 2\sqrt{\frac{S}{\pi}} \quad (1)$$

$$194 \quad R_L = \frac{2L}{\pi} \quad (2)$$

$$195 \quad C = \frac{R_S}{R_L} = \frac{\sqrt{\pi S}}{L} \quad (3)$$

196 where  $S$  is the area of the YRD,  $L$  is the length of the coastline, and  $C$  is the delta radius ratio.

197

## 198 **4. Results and discussion**

### 199 **4.1. Runoff and sediment load in the Yellow River**

200 Lijin hydrological station is located approximately 100 km upstream from the river mouth  
 201 (Figure 1a), and is the final hydrological gauging station in the Yellow River used for monitoring  
 202 the water-sediment delivery process into the Bohai Sea. In accordance with previous research  
 203 (Wang et al., 2010), we used the runoff and sediment load measured at Lijin hydrological station to  
 204 represent the delivery characteristics in the Yellow River delta lobe, noting that about 1.7 % of the  
 205 Yellow River sediment load passing Lijin is deposited in the river course before reaching the sea  
 206 (Hu and Cao, 2003). Figure 2 shows the temporal behavior of annual runoff and sediment load at  
 207 Lijin hydrological station from 1983 to 2011. During this period, the average annual runoff is  $18.0$   
 208  $\times 10^9 \text{ m}^3$  and average annual sediment load is  $341 \times 10^6 \text{ t}$ . The maximum annual values for runoff  
 209 of  $49.08 \times 10^9 \text{ m}^3$  and sediment load of  $1024 \times 10^6 \text{ t}$  occurred in 1983, and the minimum annual  
 210 values of runoff of  $1.86 \times 10^9 \text{ m}^3$  and sediment load of  $16 \times 10^6 \text{ t}$  occurred in 1997. There is a positive  
 211 linear correlation between the runoff and sediment load, with a correlation coefficient of 0.61,  
 212 which is 99 % significant. From the variations evident in the plot, the 29-year (1983-2011) series of  
 213 runoff and sediment load can be divided into three stages, i.e., before 2000, 2000-2002 and after  
 214 2002.

215

### 216 **Figure 2**

217

218 Before 2000, the runoff and sediment load in the Yellow River exhibited downward trends,  
 219 with mean runoff of  $20.2 \times 10^9 \text{ m}^3 \text{ yr}^{-1}$  and mean sediment load of  $488 \times 10^6 \text{ t yr}^{-1}$ , well below the

220 average values for the 1970s ( $31.1 \times 10^9 \text{ m}^3 \text{ yr}^{-1}$  and  $898 \times 10^6 \text{ t yr}^{-1}$  respectively). From the 1980s  
221 onwards, the strength of monsoons in China weakened substantially, leading to significant droughts  
222 in North China, and particularly affecting much of Yellow River Basin (which is located in arid and  
223 semi-arid regions). From 1983 to 2000, annual precipitation in the Yellow River Basin declined  
224 overall whilst annual temperature increased, the latter due to global warming (Figure 3). The higher  
225 temperatures significantly accelerated evaporation, resulting in further decrease in runoff (Figure  
226 2a). The large fluctuations in precipitation in the Yellow River Basin were possibly linked with El  
227 Niño/Southern Oscillation (ENSO) events (Wang et al., 2006a). Human activities also had a  
228 significant effect on runoff and sediment loads into the sea (Miao et al., 2011). The population  
229 along the Yellow River Basin swelled, causing significant increases in domestic, agricultural and  
230 industrial water consumption (Peng et al., 2010). Water was wasted through poor irrigation and  
231 relatively unregulated land-use practices. A direct consequence of the reduced precipitation and  
232 increased water abstraction was the drying up of the Yellow River, experienced as no-flow events  
233 (Figure 4). Hydrological records from Lijin hydrological station show that the total of seasonal  
234 no-flow events along the Yellow River channel reached 940 days after 1982, including 901 days in  
235 the 1990s. The most serious series of droughts in the Yellow River occurred in 1997, when no-flow  
236 events occupied a total of 226 days (Figure 4), resulting from far below normal rainfall and runoff  
237 in the Yellow River basin (Figure 2).

238

239 **Figure 3**240 **Figure 4**

241

242 No further no-flow events have been recorded along the Yellow River from 2000 to date. In  
243 the period from 2000-2002, the amounts of runoff and sediment load entering the sea remained at  
244 low levels. The mean runoff of  $4.57 \times 10^9 \text{ m}^3 \text{ yr}^{-1}$  and mean sediment load of  $32 \times 10^6 \text{ t yr}^{-1}$   
245 corresponded to 77 % and 93 % reductions compared to their counterpart values in the period from  
246 1983-2000. In addition to the decline in precipitation, the construction and operation of large  
247 reservoirs played a significant role during the second stage from 2000 to 2002. By 2001, more  
248 than 3,147 reservoirs had been built in the Yellow River Basin, with a total storage capacity of  $57.4$   
249  $\times 10^9 \text{ m}^3$  (Zhang et al., 2001). Of these, the Xiaolangdi Reservoir had the greatest effect (Zhang et  
250 al., 2011). The Xiaolangdi Reservoir (Figure 1a) became operational during 1999-2001, with a total

251 storage capacity of  $12.7 \times 10^9 \text{ m}^3$ . During this period, Xiaolangdi's primary operating mode  
252 involved water storage and sediment retention (Figure 5b), greatly reducing the runoff and  
253 sediment load reaching the YRD. Since 2002, the Yellow River Conservancy Commission (YRCC)  
254 has performed more than 10 flushing operations to regulate the flow of water and sediment into the  
255 lower reaches of the Yellow River through the coordinated operation of Xiaolangdi and other  
256 reservoirs (Table 2). The regulation primarily involved release of water stored upstream of the  
257 Xiaolangdi dam to scour sediment that had been accreting on the bed of the downstream channel,  
258 and hence control the flood risk posed by the resulting 'hanging river'. These regulation measures  
259 had a direct impact on hydrological processes in the drainage area of the lower Xiaolangdi  
260 catchment, and also influenced the river flux delivery to the Bohai Sea .

261

262

**Table 2**

263

**Figure 5**

264

265 After 2003, the runoff and sediment load maintained higher values than in the second stage,  
266 with a mean annual runoff of  $18.33 \times 10^9 \text{ m}^3 \text{ yr}^{-1}$  and a mean annual sediment load of  $167 \times 10^6 \text{ t}$   
267  $\text{yr}^{-1}$ . Relative to the first stage, the runoff essentially returned to the same level to that of the  
268 mid-1990s, whereas the sediment load remained at low values, steadily decreasing with time. This  
269 behavior is primarily due to the water and sediment regulation activities at Xiaolangdi, along with  
270 the soil and water conservation efforts along the middle reaches of the Yellow River.

271

272

273

274

275

276

277

278

279

280

281

At Sanmenxia hydrological station, both the annual runoff and sediment load decreased  
significantly with time (Figure 5), indicating the effectiveness of the soil and water conservation  
and ecological restoration practices implemented on the Loess Plateau. The variations in runoff  
about the trend may be attributed to variations in the monsoon climate during the wet season  
promoted by El Niño/Southern Oscillation (ENSO) events. Compared to Sanmenxia station,  
Huayuankou experienced a lower sediment load and a higher level of runoff over time (Figure 5).  
From 1983-1999, the annual average runoff increased by 9% and annual average sediment load  
reduced by 13% at Huayuankou relative to Sanmenxia. From 2003-2011, the annual average runoff  
at Huayuankou increased by 17% and the annual average sediment load reduced by 67% compared  
with Sanmenxia. These results demonstrate that the construction and operation of the Xiaolangdi  
Reservoir played a significant role in water and sediment regulation of the lower Yellow River

282 (Table 2). Although each water and sediment regulation activity typically lasted about one month,  
283 the effect on sediment transport was huge. By 2011, the water and sediment discharges due to  
284 regulation activities accounted for 27% and 42% of the total discharges, indicating that the  
285 sediment transport capacity had been significantly improved. The foregoing analysis highlights the  
286 increasingly prominent impact of human activities on runoff and sediment loads.

287

## 288 4.2 The Evolution of the Yellow River Delta from 1983 to 2011

### 289 4.2.1 Area changes

290 Figure 6 shows the annual values of plan-form area of the YRD as a function of year from  
291 1983 to 2011. It can be discerned that the YRD increased in area by about 248 km<sup>2</sup> during the study  
292 period. The changing area exhibits three trends; a steady increase from 1983 to 2000 when the area  
293 reached a peak value of 3,924 km<sup>2</sup>; a rapid decrease at a rate of 68 km<sup>2</sup> yr<sup>-1</sup> from 2000 to 2003, and  
294 then a more gradual increase from 2003 onwards (Figure 6). We therefore divide the area changes  
295 into a rapid growth stage (1983-2000), a retreat stage (2000-2003), and a recovery stage  
296 (2003-2011), all in response to the variations in runoff and sediment load. The rapid growth stage  
297 was dominated by the twin effects of drought and excess water consumption. The retreat stage  
298 coincided with the reservoir at Xiaolangdi initially becoming operational, and the implementation  
299 of water conservation measures and improved irrigation and land-use. The recovery stage indicates  
300 that the measures may not have been sufficient to prevent further growth of the delta, and may be  
301 linked to the development of the new delta lobe at Qing 8 that was initially created in 1996.

302

303

### 303 **Figure 6**

304

305 Figure 7 presents satellite images in selected years, highlighting the changing shape of the  
306 Yellow River Delta with time. Figure 8 shows the migration of the Yellow River Delta coastline  
307 from 1983 to 2011. From 1983 to 1996, the delta lobe of the YRD evolved forward at a mean rate  
308 of 20.97 km<sup>2</sup> yr<sup>-1</sup> as an extension of the Qingshuigou channel (Figure 7A-G). From Figure 8A it can  
309 be deduced that the growing delta lobe progressed forward at an average rate of 1.4 km yr<sup>-1</sup>. By  
310 1996, an obvious promontory had formed (Figure 7G). After 1996, the shoreline and area started to  
311 extend forward as a new delta lobe in the northeast direction along the Qing 8 channel. Meanwhile

312 the old Qingshuigou promontory began to retreat because of net erosion once the water and  
313 sediment supply became cut off (Figure 7H-O and Figure 8A). From 1997 to 2000, the YRD  
314 continued to evolve, with simultaneous extension of the Qing 8 delta lobe and erosion of the  
315 Qingshuigou promontory. Apart from sediment load, several other factors influence the short-term  
316 evolution of a delta, including sediment grain size (Edmonds and Slingerland, 2007), sediment  
317 cohesion (Edmonds and Slingerland, 2010), sediment feed point (Kim et al., 2009) and river plume  
318 behavior (Falcini et al., 2012). Given that there was no significant change of river plume behavior  
319 and sediment characteristics, the drastic change in land area of the YRD in the late 1990s and early  
320 2000s was most likely due to the relatively low runoff and sediment load (Figure 2) (Liu et al.,  
321 2012a). Meanwhile, coastal erosion remained basically unchanged. Both the Qingshuigou and the  
322 Qing 8 delta lobes eroded gradually during 2000 to 2003 (Figure 8B). With the restoration of runoff  
323 and sediment load (Figure 2), the area of the YRD began to increase incrementally after 2003 (Cui  
324 and Li, 2011), the trend having a mean rate of  $17.1 \text{ km}^2 \text{ yr}^{-1}$ . Figure 8C shows the growth of the  
325 Qing 8 lobe while the old Qingshuigou lobe retreated during 2003 to 2011. Although the total  
326 plan-form area of the YRD increased by 3.7% from 2003 to 2011, the area declined by 1.7% from  
327 2000 to 2011. Fixing the annual runoff and sediment load at their 2011 values, more than a decade  
328 would be required for the YRD to recover to the area it had in 2000.

329

330 **Figure 7**331 **Figure 8**

332

333

334 **4.2.2 Coastline migration**

335 Over time, the length of coastline of the YRD increased, unlike its area (Figure 9), indicating  
336 that the coastline was becoming more and more tortuous. From 1983 to 2011, the length of the  
337 coastline increased by 36.45 km, equivalent to an average annual growth of 1.3 km. Both coastline  
338 extension and retreat occurred during this period, with a coefficient of variation of about 7.8 %,  
339 which is higher than the corresponding value for the land area. Comparison between the annual  
340 changes in YRD area and YRD coastline indicated that the changes were not correlated. For  
341 example, as the delta shrank, its area reduced but its shape became increasingly contorted thus  
342 increasing the length of its coastline.

343

344

**Figure 9**

345

## 346 4.2.3 Morphological changes

347 Figure 10 shows the variation with time of the delta radius ratio,  $R_S / R_L$ , which provides a  
348 measure of the evolution of the shape of the entire YRD from 1983 to 2011. Despite the  
349 considerable inter-annual fluctuations evident, the delta radius ratio exhibits a decreasing trend over  
350 time, indicating that the morphology of the YRD became increasingly irregular over the study  
351 period. Taking spot values at either end of the period, the delta radius ratio of the YRD fell from  
352 0.68 in 1983 to 0.57 in 2011. The delta radius ratio had a coefficient of variation of 7.8 %, which is  
353 very similar to that obtained for the coastline length. This is hardly surprising, given the close  
354 linkage between the morphology of the YRD and the shifts occurring to its river course and the  
355 associated dynamic changes in orientation of the delta lobe. It is well known that many factors  
356 influence the orientation of delta lobes, including near-shore currents (Li et al., 2001), Coriolis  
357 force (Fan et al., 2006a), water-sediment processes (Wang et al., 2005) and local terrain conditions.  
358 In 1983, the Qingshuigou channel mouth experienced major siltation, with the emergence of many  
359 small branch channels and sand bars separating the channels (Figure 11A). In 1984, the direction of  
360 the Qingshuigou channel mouth altered from east to southeast, and a promontory formed over the  
361 next 12 years (Figure 11B). Meanwhile, the delta radius ratio decreased from 0.68 to 0.62. After a  
362 further artificial channel diversion in 1996, a new delta lobe began rapidly to develop from the  
363 Qing 8 channel (Figure 11C). From 1996 to 2007, the YRD became more irregular, with its delta  
364 radius ratio declining from 0.62 to 0.54. Due to heavy erosion related to bank bursts, multiple  
365 branches appeared along the north side of the river mouth (Figure 11D). Excessive runoff during  
366 the flood season of 2007 caused the Qing 8 channel mouth to divert northward by 2 km. After 2007,  
367 the orientation of the Yellow River mouth continued further northward. By 2011, the direction of  
368 the river mouth was almost directly north, and the tip of the delta lobe was no longer sharp (Figure  
369 11E). This change led to a more spatially uniform development of the delta, with its radius ratio  
370 increasing from 0.54 in 2007 to 0.57 in 2011.

371

372

**Figure 10**

373

374

Figure 11

375

376 4.3 Relationship between evolution of YRD and variations in runoff and sediment load

377 Evolution of the YRD is influenced by several key factors (see e.g. Chu et al., 2006), including  
378 river discharge, sediment input, wave energy, tidal regime, littoral currents etc. Changes to any of  
379 these factors could affect the geomorphological and sedimentological regimes of the delta (Wang et  
380 al., 2010). In particular, interactions among soil, fluvial and coastal dynamics are responsible for  
381 enhancing the relative roles between sedimentation and erosion at delta lobes, thus controlling the  
382 growth and shape of the overall delta. For the YRD to be in equilibrium and its area remain  
383 constant, the rate of river sediment accumulation must equal the erosion rate due to near-shore  
384 coastal flows. When the accumulation rate of river sediment is less than the coastal erosion rate, the  
385 YRD starts to shrink and its area consequently reduces. Conversely, when the accumulation rate of  
386 river sediment is higher than the coastal erosion rate, the delta lobe extends further and the area of  
387 the YRD increases. Over the past 30 years, the near-shore coastal dynamics has hardly varied at the  
388 Yellow River mouth (Wang et al., 2010; Hu and Cao, 2003) and so changes to the river flux appear  
389 to be the key factor controlling the evolution of the delta (Fan et al., 2006b). A previous study has  
390 shown that the threshold value of river flux required to keep the YRD stable varies for different  
391 channels (Wang et al., 2006b). Obviously, the riverbed features and coastal dynamics are particular  
392 to each channel, affecting the depositional characteristics of sediment delivered into the sea.

393 Noting that the runoff and sediment reached the sea through different channels before and after  
394 the artificial diversion of the main delta lobe from Qingshuigou to Qing 8 was introduced in 1996,  
395 we carried out stepwise multiple regression analysis over two phases, 1983-1995 and 1997-2011.  
396 The regression analysis indicated that river sediment load is a dominant factor influencing the  
397 evolution of the YRD. However, taking runoff and sediment load simultaneously into account,  
398 the results from the regression analysis indicated no further contribution from runoff, which is  
399 reasonable given the significant correlation between the annual sediment load and annual runoff.  
400 Here, we define the annual area change in the  $i+1$  th year as the arithmetic difference between the  
401 area of the YRD in the  $i+1$  th year minus that in the  $i$  th year. The linear regression functions  
402 obtained between the annual sediment load ( $x$ ,  $10^9$  t) and the annual change in area of YRD ( $y$ ,  $\text{km}^2$ )  
403 for the two phases before and after 1996 are:

$$404 \quad y = 0.1758x - 77.466 \quad R^2 = 0.3 \quad P = 0.0 \quad \text{before 1996} \quad (4)$$

$$405 \quad y = 0.3317x - 52.8 \quad R^2 = 0.4 \quad P = 0.0 \quad \text{after 1996} \quad (5)$$

406 Figure 12 plots the YRD area change against sediment load along with the regression lines, for both  
 407 phases. Although scatter is evident, the trends are of increasing area changes with sediment load.  
 408 Using equations (4) and (5), the annual change in area of YRD is zero and equilibrium is achieved  
 409 when the average annual sediment load equals  $441 \times 10^6$  t in 1983-1995 and  $159 \times 10^6$  t in  
 410 1997-2011. These threshold values of sediment load are substantially different, demonstrating again  
 411 the important influence of the river flux characteristics on the evolution of the delta.

412

413 Figure 12

414

## 415 4.4 Error analysis

416 The exact position of the coastline of YRD varies with time and tide, and so errors are  
 417 introduced to the analysis when comparing coastlines extracted from satellite images acquired at  
 418 different times in any given day. Although researchers initially held the view that the tidal effect is  
 419 weak and can be ignored for the Yellow River estuary (Chu et al., 2006), more recently Liu et al.  
 420 (2012b) reported that tidal and landform variations can have a significant influence on the detection  
 421 of coastline changes in the Yellow River delta. Liu et al. evaluated the maximum error caused by  
 422 the tidal effects, assuming that the entire coastline remains parallel under different tidal conditions,  
 423 and regarding the error in delta area as the product of the maximum coastline distance and coastline  
 424 length. Liu et al. then found the maximum distance among the coastlines for YRD in the same day  
 425 is less than 172 m. In the present study, the extracted total coastline length and delta area are less  
 426 than 210 km (Figure 9) and  $3950 \text{ km}^2$  (Figure 6), and so, using the foregoing method, the maximum  
 427 relative error is about 1.1 % of the total delta area. Table 3 lists the relative error in the annual  
 428 extracted delta area.

429

430 **5. Conclusions**

431 Previous studies have identified climate change and local human activities as two primary factors  
 432 that impact on the evolution of river deltas. This paper has focused on recent changes taking place  
 433 to the Yellow River delta. We found that the runoff and sediment load at the mouth of the Yellow

434 River exhibited downward trends with great inter-annual variations during the period from 1983 to  
435 2011. These temporal variations in runoff and sediment load directly affected the evolution of the  
436 YRD, including its area change, shoreline migration and morphology. The downward trends in  
437 runoff were linked to progressively reduced precipitation due to climate warming, and increasing  
438 water consumption connected with poor irrigation practice and rapid socio-economic development.  
439 The trends in sediment load are largely due to soil conservation measures including 100,000 check  
440 dams along the main river and the reduced sediment carrying capacity of the river due to the  
441 reduced runoff. The inter-annual fluctuations have been previously related to El Niño/Southern  
442 Oscillation (ENSO) events affecting monsoon rainfall in the upper Yellow River catchment. Over  
443 the time period considered, the area of the YRD underwent three stages of evolution: a rapid  
444 growth stage (1983-2000), a retreat stage (2000-2003) and a recovery stage (2003-2011). Operation  
445 of the Xiaolangdi reservoir and implementation of new water consumption policies by the Yellow  
446 River Conservancy Commission helped drive changes to the delta area during the retreat and  
447 recovery stages. From 1983 to 2011, the delta area increased by 248 km<sup>2</sup> and its coastline grew by  
448 36.45 km in length. During this period, the shape of the entire YRD became more and more  
449 irregular because of the emergence of the Qingshuigou and the Qing 8 delta lobes. Multi-step  
450 regression analysis indicated that average river sediment loads of  $\sim 441 \times 10^6 \text{ t yr}^{-1}$  and  $159 \times 10^6 \text{ t yr}^{-1}$   
451 would have been necessary to maintain equilibrium of the YRD area in the periods where the main  
452 delta lobe followed the Qingshuigou route in 1983-1996 and the Qing 8 route in 1996-2011.

#### 453 **Acknowledgments**

454 Funding for this research was provided by the Open Foundation of Key Laboratory of Soil and  
455 Water Loss Process and Control on the Loess Plateau of Ministry of Water Resources (2014005),  
456 the National Natural Science Foundation of China (no. 41001153), Beijing Higher Education  
457 Young Elite Teacher Project and State Key Laboratory of Earth Surface Processes and Resource  
458 Ecology.

459

#### 460 **References**

- 461 Chander, G., Markham, B.L., Helder, D.L., 2009. Summary of current radiometric calibration  
462 coefficients for Landsat MSS, TM, ETM+, and EO-1 ALI sensors. Remote sensing of  
463 environment, 113(5): 893-903.
- 464 Chen, J., Wang, S., Mao, Z., 2011. Monitoring wetland changes in Yellow River Delta by remote

- 465 sensing during 1976-2008. *Progress in Geography*, 30(05): 585-592.
- 466 Chu, Z.X., Sun, X.G., Zhai, S.K., Xu, K.H., 2006. Changing pattern of accretion/erosion of the  
467 modern Yellow River (Huanghe) subaerial delta, China: Based on remote sensing images.  
468 *Marine Geology*, 227(1-2): 13-30.
- 469 Cui, B., Li, X., 2011. Coastline change of the Yellow River estuary and its response to the sediment  
470 and runoff (1976–2005). *Geomorphology*, 127(1-2): 32-40.
- 471 Cui, B., Yang, Q., Yang, Z., Zhang, K., 2009. Evaluating the ecological performance of wetland  
472 restoration in the Yellow River Delta, China. *Ecological Engineering*, 35(7): 1090-1103.
- 473 Cui, G., Zhang, X., Zhang, Z., Xu, Z., 2013. Changes of coastal wetland ecosystems in the Yellow  
474 River Delta and protection countermeasures to them. *Asian Agricultural Research*, 5(1):  
475 48-50.
- 476 Del Frate, F., Latini, D., Minchella, A., Palazzo, F., 2012. A new automatic technique for coastline  
477 extraction from SAR images, *SPIE Remote Sensing*. International Society for Optics and  
478 Photonics, 8536:85360R.
- 479 Dellepiane, S., De Laurentiis, R., Giordano, F., 2004. Coastline extraction from SAR images and a  
480 method for the evaluation of the coastline precision. *Pattern Recognition Letters*, 25(13):  
481 1461-1470.
- 482 Edmonds, D.A., Slingerland, R.L., 2007. Mechanics of river mouth bar formation: Implications for  
483 the morphodynamics of delta distributary networks. *Journal of Geophysical Research*, 112:  
484 F02034.
- 485 Edmonds, D.A., Slingerland, R.L., 2010. Significant effect of sediment cohesion on delta  
486 morphology. *Nature Geoscience*, 3(2): 105-109.
- 487 El Banna, M.M., Frihy, O.E., 2009. Human-induced changes in the geomorphology of the  
488 northeastern coast of the Nile delta, Egypt. *Geomorphology*, 107(1-2): 72-78.
- 489 Falcini, F. et al., 2012. Linking the historic 2011 Mississippi River flood to coastal wetland  
490 sedimentation. *Nature Geoscience*, 5(11): 803-807.
- 491 Fan, H., Huang, H., Zeng, T., 2006a. Impacts of anthropogenic activity on the recent evolution of  
492 the Huanghe (Yellow) River Delta. *Journal of coastal research*, 22(4): 919-929.
- 493 Fan, H., Huang, H., Zeng, T.Q., Wang, K., 2006b. River mouth bar formation, riverbed aggradation  
494 and channel migration in the modern Huanghe (Yellow) River delta, China.  
495 *Geomorphology*, 74: 124-136.

- 496 Fang, H., Liu, G., Kearney, M., 2005. Georelational analysis of soil type, soil salt content, landform,  
497 and land use in the Yellow River Delta, China. *Environmental management*, 35(1): 72-83.
- 498 Gao, Y., Zhu, B., Wang, T., Wang, Y.F., 2012. Seasonal change of non-point source  
499 pollution-induced bioavailable phosphorus loss: a case study of Southwestern China.  
500 *Journal of Hydrology*, 420-421: 373-379
- 501 Gao, Y., et al., 2014a. Phosphorus and carbon competitive sorption-desorption and associated  
502 non-point loss respond to natural rainfall events. *Journal of Hydrology*, 517:447-457.
- 503 Gao, Y., et al., 2014b. Water use efficiency threshold for terrestrial ecosystem carbon sequestration  
504 under afforestation in China. *Agricultural and Forest Meteorology*, 195-196, 32-37.
- 505 Geleynse, N., Voller, V.R., Paola, C., Ganti, V., 2012. Characterization of river delta shorelines.  
506 *Geophysical Research Letters*, 39(17): L17402.
- 507 Higgins, S., Overeem, I., Tanaka, A., Syvitski, J.P.M., 2013. Land subsidence at aquaculture  
508 facilities in the Yellow River delta, China. *Geophysical Research Letters*, 40(15):  
509 3898-3902.
- 510 Hu, C., Cao, W., 2003. Variation, regulation and control of flow and sediment in the Yellow River  
511 Estuary: I. Mechanism of flow-sediment transport and evolution. *Journal of Sediment  
512 Research*, 5: 1-8.
- 513 Jiang, D., Fu, X., Wang, K., 2013. Vegetation dynamics and their response to freshwater inflow and  
514 climate variables in the Yellow River Delta, China. *Quaternary International*, 304: 75-84.
- 515 Kim, W., Dai, A., Muto, T., Parker, G., 2009. Delta progradation driven by an advancing sediment  
516 source: Coupled theory and experiment describing the evolution of elongated deltas. *Water  
517 Resources Research*, 45(6): W06428.
- 518 Le, T.V.H., Nguyen, H.N., Wolanski, E., Tran, T.C., Haruyama, S., 2007. The combined impact on  
519 the flooding in Vietnam's Mekong River delta of local man-made structures, sea level rise,  
520 and dams upstream in the river catchment. *Estuarine, Coastal and Shelf Science*, 71(1-2):  
521 110-116.
- 522 Lee, J. S., Jurkevich, I., 1990. Coastline detection and tracing in SAR images. *Geoscience and  
523 Remote Sensing, IEEE Transactions on*, 28(4): 662-668.
- 524 Li, G., Tang, Z., Yue, S., Zhuang, K., Wei, H., 2001. Sedimentation in the shear front off the Yellow  
525 River mouth. *Continental Shelf Research*, 21(6-7): 607-625.
- 526 Li, G., Wei, H., Han, Y., Chen, Y., 1998. Sedimentation in the Yellow River delta, part I: flow and

- 527 suspended sediment structure in the upper distributary and the estuary. *Marine Geology*,  
528 149(1): 93-111.
- 529 Li, G. 2003 Ponderation and Practice of the Yellow River Control, Yellow River Conservancy  
530 Press.
- 531 Lim D.I., Jung H.S., Choi J.Y., Yang S., and Ahn K.S., 2006. Geochemical compositions of river  
532 and shelf sediments in the Yellow Sea: Grain-size normalization and sediment provenance.  
533 *Continental Shelf Research*, 26: 15-24
- 534 Liu, F., Chen, S., Peng, J., Chen, G., 2012a. Temporal variations of water discharge and sediment  
535 load of Huanghe River, China. *Chinese Geographical Science*, 22(5): 507-521.
- 536 Liu, H., Jezek, K.C., 2004. Automated extraction of coastline from satellite imagery by integrating  
537 Canny edge detection and locally adaptive thresholding methods. *International Journal of*  
538 *Remote Sensing*, 25(5): 937-958.
- 539 Liu, Y., Huang, H., Qiu, Z., Chen, J., Yang, X., 2012b. Monitoring Change and Position of  
540 Coastlines from Satellite Images Using Slope Correction in a Tidal Flat: A Case Study in  
541 the Yellow River Delta. *Acta Geographica Sinica*, 67(3): 377-387.
- 542 Liu, Y., Huang, H., Qiu, Z., Fan, J., 2013. Detecting coastline change from satellite images based  
543 on beach slope estimation in a tidal flat. *International Journal of Applied Earth Observation*  
544 *and Geoinformation*, 23: 165-176.
- 545 Mason, D.C., Davenport, I.J., 1996. Accurate and efficient determination of the shoreline in ERS-1  
546 SAR images. *Geoscience and Remote Sensing, IEEE Transactions on*, 34(5): 1243-1253.
- 547 Miao, C., Shi, W., Chen, X., Yang, L., 2012a. Spatio-temporal variability of streamflow in the  
548 Yellow River: possible causes and implications. *Hydrological Sciences Journal*, 57(7):  
549 1355-1367.
- 550 Miao, C.Y., Ni J.R. Borthwick A.G.L., Yang, L., 2011. A preliminary estimate of human and natural  
551 contributions to the changes in water discharge and sediment load in the Yellow River.  
552 *Global and Planetary Change*, 76(3-4): 196-205.
- 553 Miao, C.Y., Ni J.R., 2009. Variation of Natural Streamflow since 1470 in the Middle Yellow River,  
554 China. *International Journal of Environmental Research and Public Health*, 6(11):  
555 2849-2864.
- 556 Miao, C.Y., Yang L., Chen, X.H., 2012b. The vegetation cover dynamics (1982–2006) in different  
557 erosion regions of the Yellow River Basin, China. *Land Degradation & Development*,

- 558 23(1): 62-71.
- 559 Miao, C.Y., Ni J.R. Borthwick A.G.L., 2010. Recent changes of water discharge and sediment load  
560 in the Yellow River basin, China. *Progress in Physical Geography*, 34(4):541-561.
- 561 Mikhailova, M., 2003. Transformation of the Ebro River Delta under the impact of intense  
562 human-induced reduction of sediment runoff. *Water Resources*, 30(4): 370-378.
- 563 Milliman, J.D., Meade, R.H., 1983. World-wide delivery of river sediment to the oceans. *The*  
564 *Journal of Geology*, 91(81): 1-21.
- 565 Ottinger, M., Kuenzer, C., Liu, G., Wang, S., Dech, S., 2013. Monitoring land cover dynamics in  
566 the Yellow River Delta from 1995 to 2010 based on Landsat 5 TM. *Applied Geography*, 44:  
567 53-68.
- 568 Peng, J., Chen, S., Dong, P., 2010. Temporal variation of sediment load in the Yellow River basin,  
569 China, and its impacts on the lower reaches and the river delta. *Catena*, 83(2-3): 135-147.
- 570 Ryan, T., Sementilli, P., Yuen, P., Hunt, B., 1991. Extraction of shoreline features by neural nets and  
571 image processing. *Photogrammetric Engineering and Remote Sensing*, 57(7): 947-955.
- 572 Snedden, G. A., Cable, J. E., Swarzenski, C., Swenson, E. 2007. Sediment discharge into a  
573 subsiding Louisiana deltaic estuary through a Mississippi River diversion. *Estuarine*  
574 *Coastal and Shelf Science*, 71(1-2), 181-193
- 575 Sun, T., Paola, C., Parker, G., Meakin, P., 2002. Fluvial fan deltas: Linking channel processes with  
576 large-scale morphodynamics. *Water Resources Research*, 38(8): 1151.
- 577 Sun Q.H., et al., 2014. Would the 'real' observed dataset stand up? A critical examination of eight  
578 observed gridded climate datasets for China. *Environmental Research Letters*, 9, 015001  
579 doi:10.1088/1748-9326/9/1/015001.
- 580 Syvitski, J.P. et al., 2009. Sinking deltas due to human activities. *Nature Geoscience*, 2(10):  
581 681-686.
- 582 Syvitski, J.P., Saito, Y., 2007. Morphodynamics of deltas under the influence of humans. *Global*  
583 *and Planetary Change*, 57(3): 261-282.
- 584 Tucker, C.J., Grant, D.M., Dykstra, J.D., 2004. NASA's global orthorectified Landsat data set.  
585 *Photogrammetric engineering and remote sensing*, 70(3): 313-322.
- 586 Wang, H. et al., 2010. Recent changes in sediment delivery by the Huanghe (Yellow River) to the  
587 sea: Causes and environmental implications in its estuary. *Journal of Hydrology*, 391(3-4):  
588 302-313.

- 589 Wang, H., Yang, Z., Bi, N., Li, H., 2005. Rapid shifts of the river plume pathway off the Huanghe  
590 (Yellow) River mouth in response to water-sediment regulation scheme in 2005. Chinese  
591 Science Bulletin, 50(24): 2878-2884.
- 592 Wang, H., Yang, Z., Saito, Y., Liu, J.P., Sun, X., 2006a. Interannual and seasonal variation of the  
593 Huanghe (Yellow River) water discharge over the past 50 years: Connections to impacts  
594 from ENSO events and dams. Global and Planetary Change, 50(3-4): 212-225.
- 595 Wang, S., Hassan, M.A., Xie, X., 2006b. Relationship between suspended sediment load, channel  
596 geometry and land area increment in the Yellow River Delta. Catena, 65(3): 302-314.
- 597 Wang, S., Yan, M., Yan, Y., Shi, C., He, L., 2012. Contributions of climate change and human  
598 activities to the changes in runoff increment in different sections of the Yellow River.  
599 Quaternary International, 282: 66-77.
- 600 Xu J. X., 2000. Grain-size characteristics of suspended sediment in the Yellow River, China, Catena,  
601 38(3): 243-263.
- 602 Xu, J., 2005. The water fluxes of the Yellow River to the sea in the past 50 years, in response to  
603 climate change and human activities. Environmental management, 35(5): 620-631.
- 604 Xu, X., Guo, H., Chen, X., Lin, H., Du, Q., 2002. A multi-scale study on land use and land cover  
605 quality change: the case of the Yellow River Delta in China. GeoJournal, 56(3): 177-183.
- 606 Yang, S.L., Milliman, J.D., Li, P., Xu, K., 2011. 50,000 dams later: Erosion of the Yangtze River  
607 and its delta. Global and Planetary Change, 75(1-2): 14-20.
- 608 Yang, W., 2012. Shifting of coastline and evolution of tidal flat in modern Yellow River Delta.  
609 Marine Geology Frontiers, 28(07): 17-23.
- 610 Yang, Z., Milliman, J., Galler, J., Liu, J., Sun, X., 1998. Yellow River's water and sediment  
611 discharge decreasing steadily. Eos, Transactions American Geophysical Union, 79(48):  
612 589-592.
- 613 Yu, J. et al., 2011. Effects of water discharge and sediment load on evolution of modern Yellow  
614 River Delta, China, over the period from 1976 to 2009. Biogeosciences, 8(9): 2427-2435.
- 615 Yu, L., 2002. The Huanghe (Yellow) River: a review of its development, characteristics, and future  
616 management issues. Continental Shelf Research, 22(3): 389-403.
- 617 Zhang, G., Wang, L., Liu, D., 1998. Biodiversity and Its conservation in the Yellow River Delta  
618 Nature Reserve ( In Chinese ). Rural Eco-Environment, 14: 16-18.
- 619 Zhang, T. et al., 2011. Assessing impact of land uses on land salinization in the Yellow River Delta,

- 620           China using an integrated and spatial statistical model. *Land Use Policy*, 28(4): 857-866.
- 621   Zhang, W., Ruan, X. H., Zheng, J. H., Zhu, Y. L., Wu, H. X. 2010. Long-term change in tidal  
622           dynamics and its cause in the Pearl River Delta, China. *Geomorphology*, 120(3-4),  
623           209-223.
- 624   Zhang, X., Wang, L., Si, F., 2001. Prediction of water consumption in the Huanghe river basin.  
625           *Water Resources and Hydropower Technology*, 6: 8-13.
- 626
- 627

ACCEPTED MANUSCRIPT

628

Table 1. List of satellite images used in the present work.

Acquisition data	Image type	Resolution (m)	Bands	Acquisition date	Image type	Resolution (m)	Bands
07/07/1983	MSS	80	4	09/08/1998	TM	30	7
07/06/1984	MSS	80	4	06/04/1999	TM	30	7
06/09/1985	TM	30	7	08/04/2000	TM	30	7
08/08/1986	TM	30	7	06/06/2001	ETM+	30	8
08/06/1987	TM	30	7	29/09/2002	ETM+	30	8
10/06/1988	TM	30	7	07/08/2003	TM	30	7
15/07/1989	TM	30	7	05/05/2004	TM	30	7
16/06/1990	TM	30	7	03/07/2005	ETM+	30	8
06/08/1991	TM	30	7	04/06/2006	ETM+	30	8
07/07/1992	TM	30	7	07/06/2007	ETM+	30	8
08/06/1993	TM	30	7	12/08/2008	ETM+	30	8
30/08/1994	TM	30	7	07/08/2009	TM	30	7
18/09/1995	TM	30	7	11/09/2010	TM	30	7
02/07/1996	TM	30	7	02/06/2011	ETM+	30	8
06/08/1997	TM	30	7				

629

630

631 Table 2 Flushings of the Xiaolangdi Reservoir to regulate water discharge and sediment load

Year	Released water discharge ( $10^9 \text{ m}^3$ )	Proportion of water discharge released for total delivery to the sea (%)	Proportion of Released sediment load ( $10^6 \text{ t}$ )	Proportion of sediment load released for total delivery to the sea (%)
2002	2.32	55.4	50.4	92.8
2003	2.77	14.4	115.1	31.2
2004	4.73	23.8	70.7	27.4
2005	4.18	20.2	45.6	23.9
2006	4.81	25.1	64.8	43.5
2007	6.18	30.3	97.3	66.2
2008	4.18	28.7	64.9	84.2
2009	3.49	26.2	34.5	61.5
2010	9.01	46.7	70.1	41.9
2011	3.73	20.2	41.2	44.5
Total	45.39	26.8	654.6	41.9

632

633

634 Table 3. Error assessment of estimated length of coastline due to daily tidal-induced fluctuations

Year	Error (%)	Year	Error (%)
1983	0.87	1998	0.95
1984	0.92	1999	1.03
1985	0.95	2000	0.99
1986	0.86	2001	0.98
1987	0.88	2002	1.09
1988	0.86	2003	1.05
1989	0.88	2004	1.00
1990	0.97	2005	1.01
1991	0.95	2006	1.05
1992	1.06	2007	1.06
1993	0.92	2008	1.07
1994	1.00	2009	1.06
1995	0.99	2010	1.06
1996	0.91	2011	1.00
1997	1.01	-	-

635

636

637 **Figure Captions**

638 Figure 1. Location of the Yellow River Delta (a) and the study area (b).

639 Figure 2. Runoff (a) and sediment load (b) at Lijin hydrological station from 1983 to 2011.

640 Figure 3. Annual average precipitation and annual average temperature in the Yellow River Basin  
641 from 1983 to 2011.

642 Figure 4. No-flow days at Lijin of the Yellow River from 1986 to 2011.

643 Figure 5. Annual runoff (a) and sediment load (b) at the Sanmenxia and Huayuankou hydrological  
644 stations from 1983 to 2011.

645 Figure 6. Area changes to the Yellow River Delta from 1983 to 2011.

646 Figure 7. Satellite images showing changes to the Yellow River Delta in different years. The  
647 coastline is drawn on the pseudo-color image, with reference to the gray image in the upper  
648 right corner.

649 Figure 8. Coastline migration of the Yellow River Delta from 1983 to 2011.

650 Figure 9. Temporal variation of the length of Yellow River Delta coastline from 1983 to 2011.

651 Figure 10. Temporal variation of delta radius ratio for the Yellow River Delta from 1983 to 2011.

652 Figure 11. Satellite images showing the changing morphology of the Yellow River delta lobes at  
653 Qingshuigou and Qing 8 in selected years from 1983 to 2011.

654 Figure 12. Relationship between the annual sediment load and annual change of delta area: (a)  
655 before and (b) after the artificial diversion from Qingshuigou to Qing 8 in 1996.

656

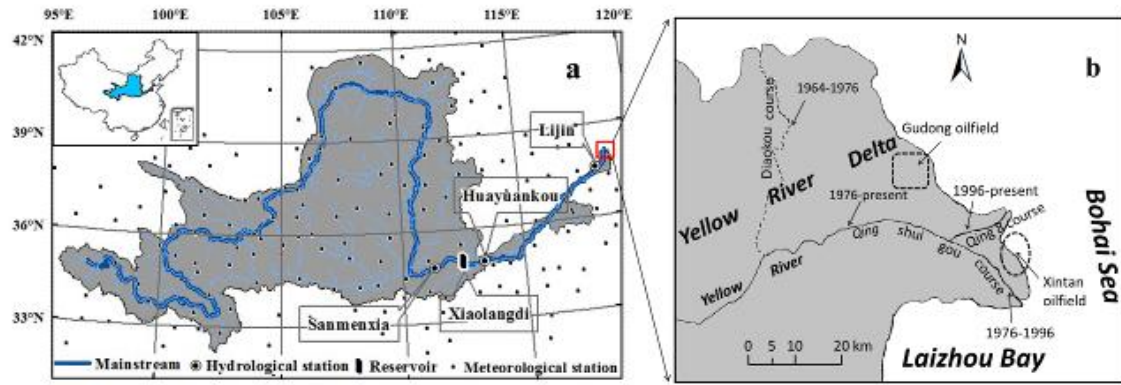
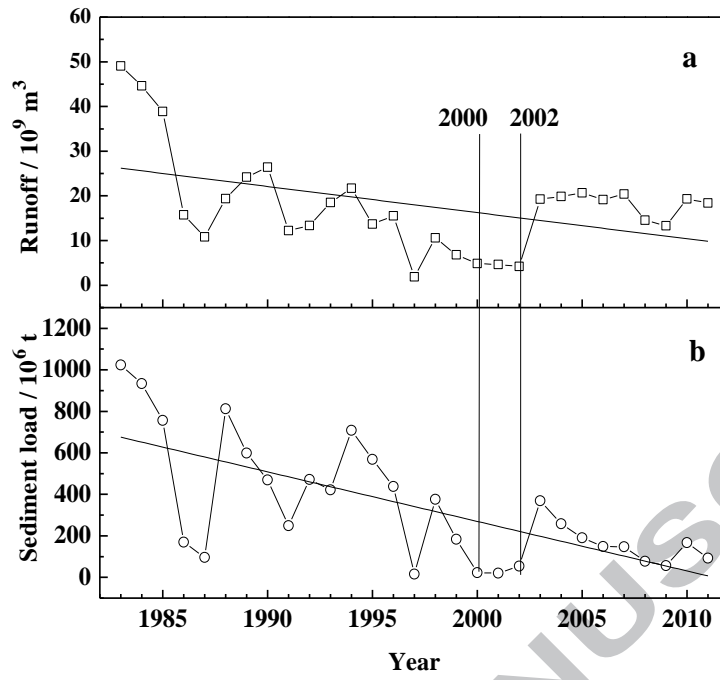


Figure 1. Location of the Yellow River Delta (a) and the study area (b).

657

658

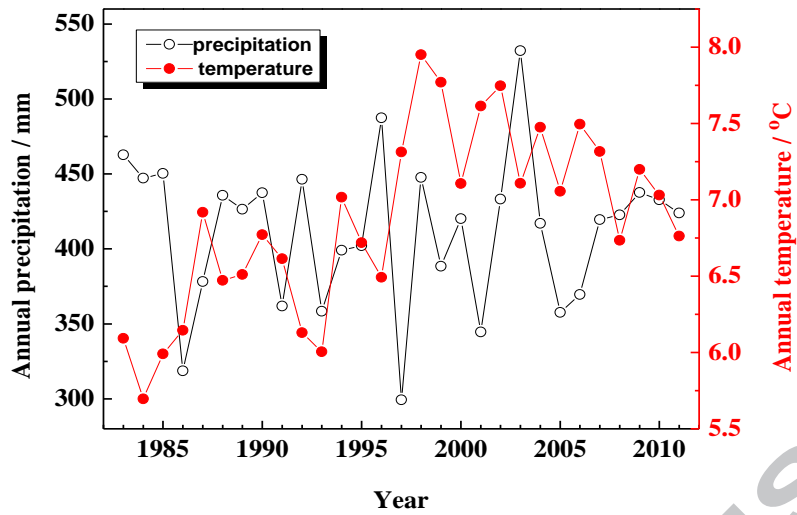
659



660

661 Figure 2. Runoff (a) and sediment load (b) at Lijin hydrological station from 1983 to 2011.

662

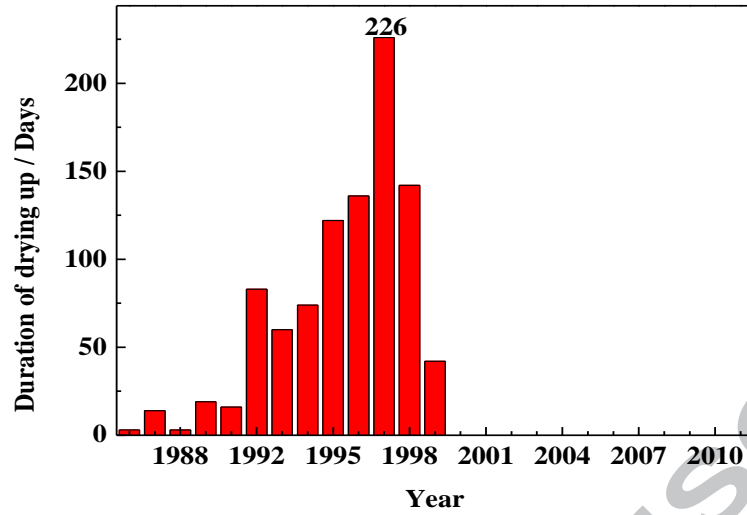


663

664 Figure 3. Annual average precipitation and annual average temperature in the Yellow River Basin

665 from 1983 to 2011.

666

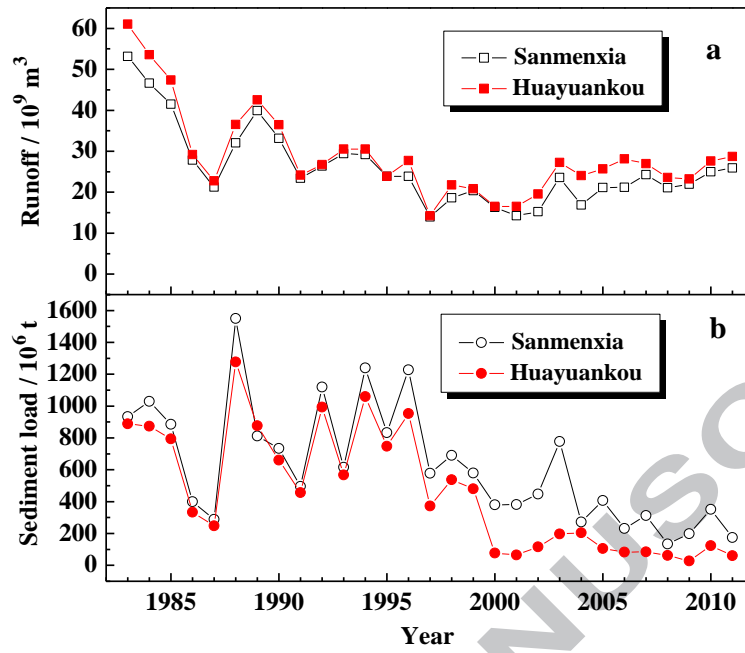


667

668

Figure 4. No-flow days at Lijin of the Yellow River from 1986 to 2011.

669



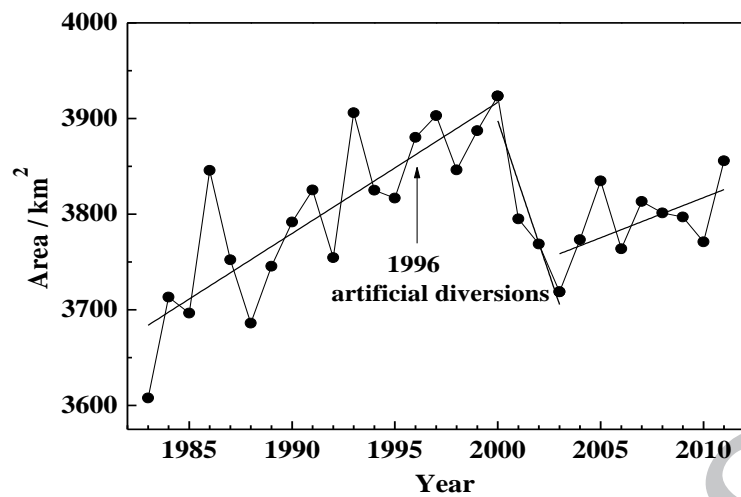
670

671 Figure 5. Annual runoff (a) and sediment load (b) at the Sanmenxia and Huayuankou hydrological

672

stations from 1983 to 2011.

673



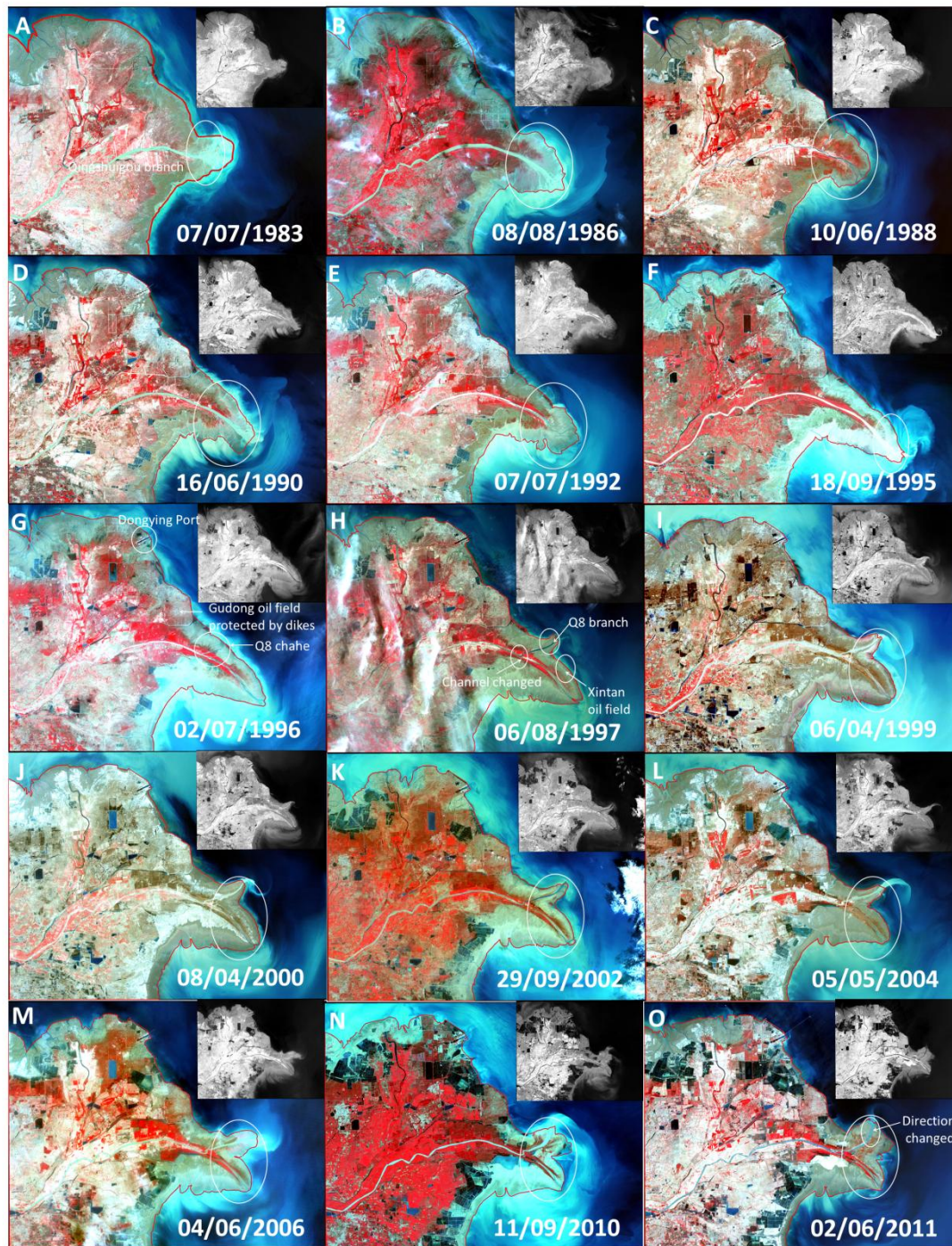
674

675

676

Figure 6. Area changes to the Yellow River Delta from 1983 to 2011.

677



678

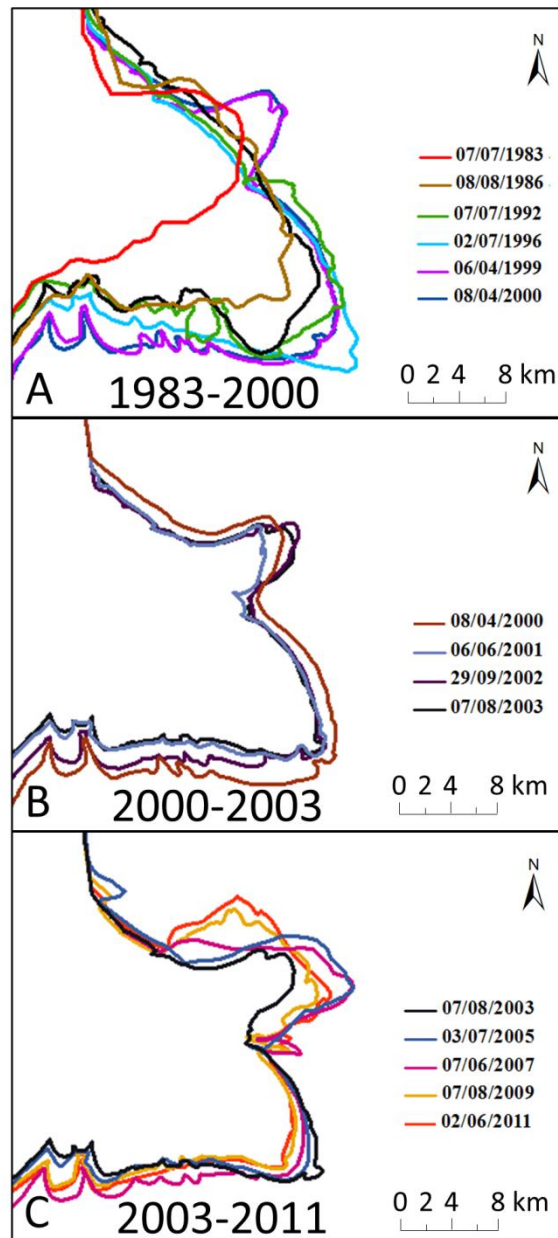
679 Figure 7. Satellite images showing changes to the Yellow River Delta in different years. The

680 coastline is drawn on the pseudo-color image, with reference to the gray image in the upper

681

right corner.

682

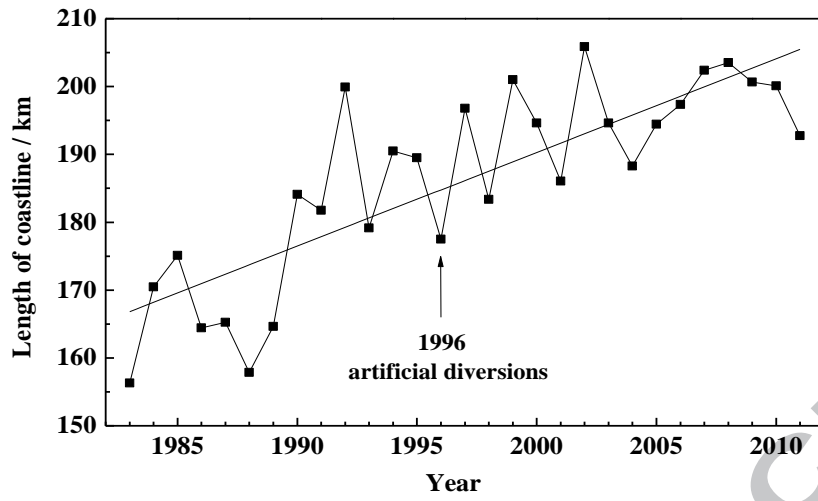


683

684

685

Figure 8. Coastline migration of the Yellow River Delta from 1983 to 2011

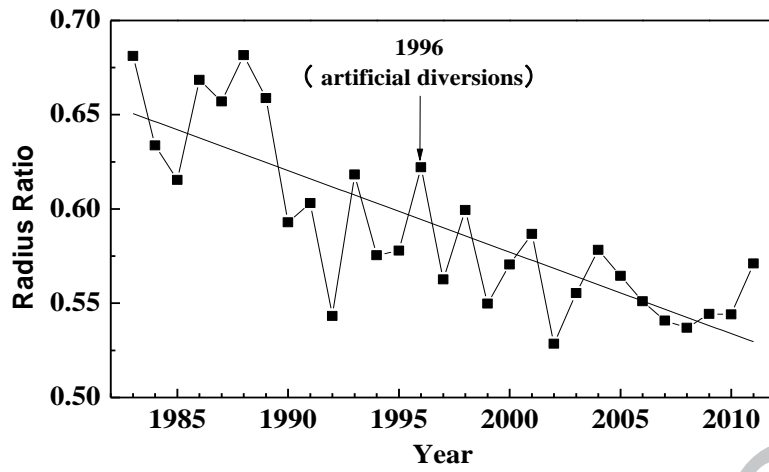


686

687

688 Figure 9. Temporal variation of the length of Yellow River Delta coastline from 1983 to 2011.

689

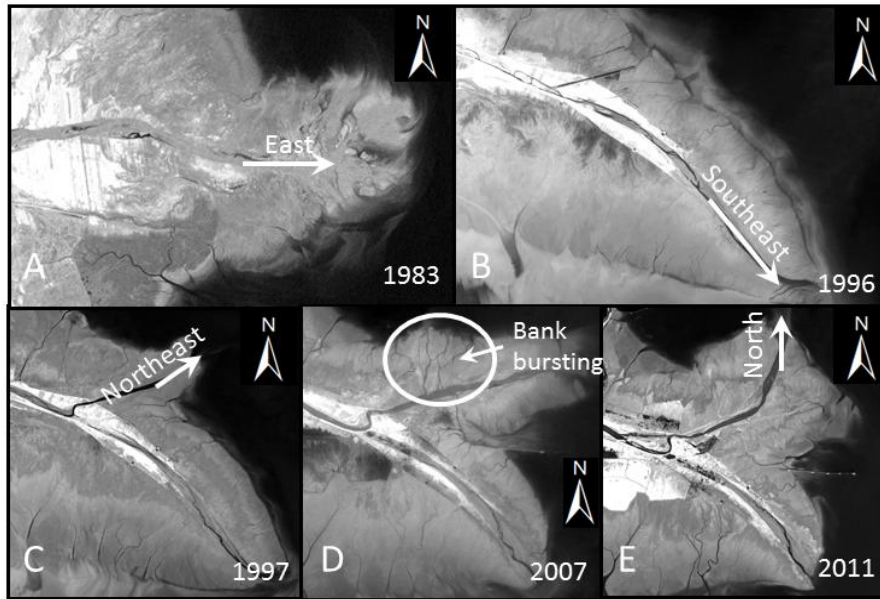


690

691

692 Figure 10. Temporal variation of delta radius ratio for the Yellow River Delta from 1983 to 2011.

693



694

695 Figure 11. Satellite images showing the changing morphology of the Yellow River delta lobes at

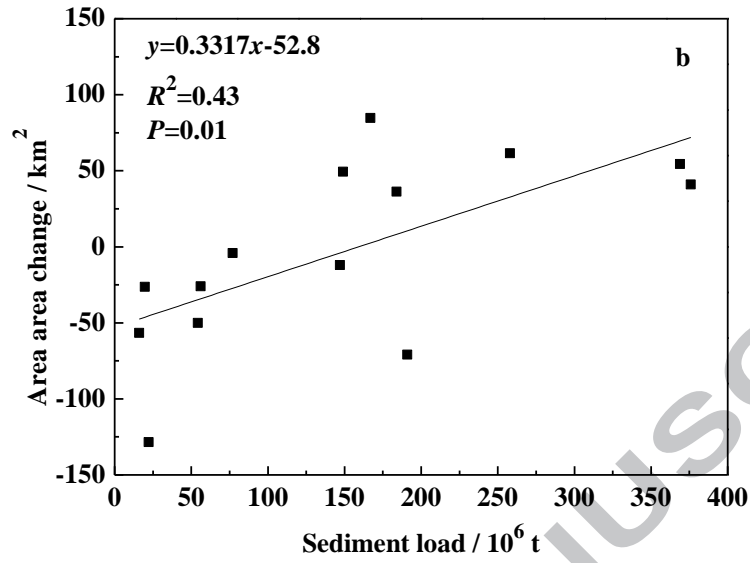
696 Qingshuigou and Qing 8 in selected years from 1983 to 2011.

697

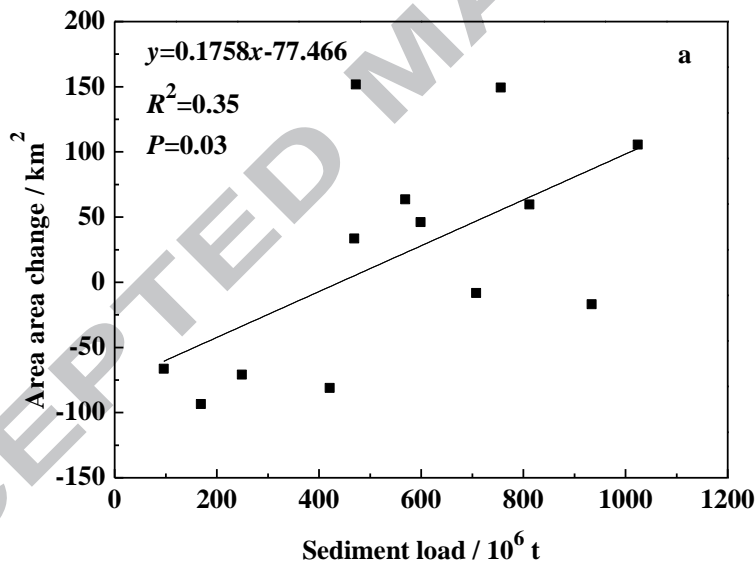
698

699

700



701



702

703 Figure 12. Relationship between the annual sediment load and annual change of delta area: (a)

704 before and (b) after the artificial diversion from Qingshuigou to Qing 8 in 1996.

705

**Highlights**

29-year satellite images were used to explore the evolution of Yellow River Delta;

The morphology of YRD is characterized by a new index defined as delta radius ratio;

The area and coastline of YRD increased by 248 km<sup>2</sup> and 36.45 km, respectively;

YRD required sediment loads of  $\sim 441 \times 10^6$  t yr<sup>-1</sup> before 1996 to maintain equilibrium;

YRD required sediment loads of  $\sim 159 \times 10^6$  t yr<sup>-1</sup> after 1996 to maintain equilibrium;

ACCEPTED MANUSCRIPT